THE DIRECTIVITY AND POLARISATION OF THICK TARGET X-RAY BREMSSTRAHLUNG FROM SOLAR FLARES

JOHN C. BROWN

*Dept. of Astronomy, University of Glasgow, Scotland**

(Received 9 May, 1972)

Abstract. The directivity and polarisation of solar hard X-ray bursts is discussed in terms of two bremsstrahlung source models. These involve continuous and impulsive injection of electrons respectively, as described widely in the literature.

A detailed analysis is made of the continuous injection model in which electrons are accelerated downward into the dense chromosphere where their velocity distribution is greatly modified by collisions. This thick target scattering is described by a simple analytical model. Directivity and polarisation of the bremsstrahlung emission are calculated in detail for a thick target model in which the guiding magnetic field is vertical.

It is predicted for this model that X-ray sources should brighten from the centre to the limb of the solar disk, while the degree of polarisation should rise from zero to around 30% near the limb. The plane of maximum intensity for any source is that containing the source and the disk centre. Both the directivity and polarisation should increase with increasing photon energy.

Very recent observations agree with these predictions though they suggest that the field is significantly non-vertical. If scattering is not included in the model, or if an impulsive injection model is taken, agreement with observations is not obtained.

1. Introduction

It is now generally accepted that solar flare hard X-ray bursts ($\gtrsim 20$ keV) are generated by collisional bremsstrahlung of non-thermal electrons (see, e.g. Korchak, 1967a; Cline *et al.*, 1968). On this basis, Korchak (1967a, b) and Elwert (1968) have proposed that the X-ray emission should in general be polarised and anisotropic due to the anisotropy likely to be present in the electron velocity distribution. Thus, observations of these effects could yield information about the electron velocity distribution in flares and so help to establish an accurate model of the X-ray source. Elwert and Haug (1970, 1971) and Haug (1972a) have performed detailed calculations of the directivity and polarisation of the emission from electrons with a power-law energy distribution moving in regions of uniform magnetic field and plasma density. These calculations include the effects of spiralling of the electrons in the field and assume idealised power-law distributions of the electrons over pitch angle. Before the results of such calculations may be usefully compared with observations, however, they must be extended to incorporate the distributions of magnetic field and plasma density likely to be present in an actual X-ray flare. In addition, where possible, pitch angle distributions derived from physical arguments should be substituted for the power-laws adopted in the work of Elwert and Haug.

* Temporarily at the Lehrstuhl für Theoretische Astrophysik der Universität Tübingen, West Germany.

Solar Physics **26** (1972) 441–459.

Two main models of hard X-ray flares appear in the literature, namely the 'impulsive injection' and 'continuous injection' models. In the impulsive model, first proposed by Takakura and Kai (1966), non-thermal electrons are accelerated, on a short time scale, in a coronal magnetic trap. Subsequently, the hard X-ray burst produced by these electrons decays due to their collisional degradation in the ambient plasma. In the continuous injection model, on the other hand, the time dependence of the X-ray intensity is determined by the modulations of a source which continuously accelerates electrons into the dense chromosphere where they rapidly decay. This latter type of model has been suggested by several authors including de Jager and Kundu (1963), Acton (1968), and Kane and Anderson (1970) and has been developed in detail by Brown (1971) and by Syrovatskii and Shmelva (1972).

Since spatial resolution of hard X-rays is at present inadequate to distinguish the geometric properties of these models, various alternative considerations have been used in attempts to eliminate one or the other. In particular, several authors (e.g. Kane and Anderson, 1970, Zirin *et al.*, 1971) have cited the fact that the impulsive model predicts a collisional hardening of the X-ray spectrum during the burst decay whereas a softening is observed (Kane and Anderson, 1970). However, Brown (1972) has shown that inclusion of the effects of a non-uniform plasma density in the trap limbs resolves this discrepancy. Considering the relevance of hard X-ray flare models to flare heating and particle acceleration processes, (Brown, 1971, 1972; Lin and Hudson, 1971; Cheng, 1972; Syrovatskii, 1972), the possibility of using directivity and polarisation measurements of X-ray bursts to distinguish the models thus assumes greater importance.

Both Ohki (1969) and Pintér (1969) have made preliminary studies of the directivity of hard X-ray bursts. On the observational side, these authors note that, although X-ray intensity measurements cannot be made for a single flare in different directions, statistical data on the directivity may be obtained from burst occurrences at different Central Meridian Distances (CMD's) on the solar disk. In this method the burst location is identified with that of the simultaneous Hα flare. On the basis of this approach Ohki (1969) and Pintér (1969) both find that the intensities vary with CMD. Drake (1971) has, however, questioned these results on the grounds that neither Ohki nor Pintér has properly corrected the burst distribution for the CMD distribution of the observed Hα flares themselves. Drake further points out that in the 1–6 keV interval, (the only range common to the studies by Ohki and by Pintér), these authors disagree on the CMD of the maximum of the burst distribution. On analysing a large sample of bursts in this energy range, with proper correction for the Hα flare distribution, Drake finds no statistically significant directivity. This result may in fact be confirmation that 1 keV X-rays are principally of thermal origin as suggested by Kahler and Kreplin (1971). Unfortunately no analysis, comparable to Drake's, seems to be available for bursts at higher (non-thermal) energies.

The first observational data on solar X-ray burst polarisation have recently been obtained by Tindo *et al.* (1970, 1972a, b) by means of the satellites Intercosmos 1 and 4. These results indicate degrees of polarisation up to about 30% at 10–20 keV, consistent with moderately anisotropic electron velocity distributions. As will be seen

later, however, in order to discriminate between X-ray source models it is also necessary to measure the orientation on the solar disk of the plane of maximum intensity (i.e. the plane of polarisation). Results of such measurements are included in the most recent paper by Tindo *et al.* (1972b) and appear to favour the continuous injection model (see Section 4). More definite conclusions should emerge from future observations showing the variation of both the degree and the plane of polarisation of bursts with X-ray energy. In addition these data, along with similar results for the directivity, could help distinguish the thermal and non-thermal X-ray components, a problem of great relevance to the energetics of the flare (Brown, 1971, 1972; Syrovatskii, 1972).

Considering the *theoretical* directivity of the emission from the continuous injection model, both Ohki (1969) and Pintér (1969) predict a maximum brightness of sources at the solar limb. Their conclusions are based on the assumption of motion of the electrons down a purely vertical field, as also assumed by Tindo *et al.* (1972b) in their discussion of the problem. However, though the electrons may indeed be *injected* down an essentially vertical field (cf. Sturrock, 1968), two factors result in considerable horizontal components of the velocity distribution in the X-ray emitting region itself. Firstly, in this model, the electrons are injected into a very dense region where they are rapidly degraded by collisions, i.e. the bremsstrahlung target is *thick*. The collisions in such a target result in a greatly modified electron beam velocity distribution. In addition to the change in the beam energy distribution as it penetrates the target (e.g. by 2 in the index of a power law energy spectrum in the electron flux – Brown, 1971), these collisions produce substantial horizontal velocity components in an initially vertical beam. Secondly, the guiding magnetic field may itself deviate considerably from the vertical in the X-ray source (cf. Strauss and Papagiannis, 1971). Thus the purely vertical electron velocities assumed by Ohki (1969) and by Pintér (1969) are not representative of the continuous injection model. Hudson (1971) has even suggested that the total absorption of the non-thermal electrons in a thick target might result in negligible directivity and polarisation of the X-ray emission. For X-ray energies well above the thermal energies of the ambient plasma particles, however, the electrons contributing to the emission will still be far from isotropic.

In analysing the impulsive model, on the other hand, Ohki (1969) and Pintér (1969) consider the electron motion as parallel to a horizontal field but the magnetic field in a coronal trap is certainly not constant in direction, being near vertical in the trap limbs (Takakura and Scalise, 1970; Benz and Gold, 1971). Emission from these limbs plays a major role in impulsive injection models, particularly at high photon energies (Brown, 1972) which are especially important in determining the directivity and polarisation of bursts (Elwert and Haug, 1971; Haug, 1972a). Furthermore the electron velocities are not even approximately parallel to the magnetic field since, in order to be trapped, the electrons must have large pitch angles.

It is evident then that, for reasonable assessment of the directivity and polarisation, more adequate representations of the two source models are necessary than those adopted by Ohki and by Pintér. The more detailed type of calculation performed by

Elwert and Haug (1971) and by Haug (1972a) is, on the other hand, applicable only to small parts of the source region over which the idealisations of uniform field and density are valid. Haug (1972a) has suggested the possibility of using these latter calculations in conjunction with magnetogram and hard X-ray polarisation measurements at high spatial resolution to test source models. At present, however, there is little likelihood of making such observations at high (non-thermal) photon energies, especially in the brief flash phase of the flare during which particle acceleration occurs. It therefore seems most valuable to proceed by extending the calculations of Elwert and Haug (1971) and Haug (1972a) to incorporate distributions of field and density representative of those in the two source models. Additionally, where possible, realistic pitch angle distributions must be derived and included in the models. In particular, the pitch angle distribution will be energy dependent in both models due to the nature of the acceleration process in impulsive models (Brown, 1972) and to the energy dependence of scattering in thick target models (see Section 2).

Non-uniformities of the magnetic field will be most important in impulsive models while non-uniform density and collisional scattering will be the main effects in continuous injection models. In this paper detailed calculations of the directivity and polarisation of a continuous injection model are made on the assumption of a purely vertical field. Non-uniform plasma density and a thick-target scattering model (obtained in Section 2) are, however, incorporated in the calculations and the consequences of a non-vertical field are discussed in Section 4.

2. Electron Scattering and Energy Loss in a Thick Target

In the dense chromospheric plasma constituting the thick target, the continuously injected electrons will lose energy predominantly by collisions (see e.g. Brown, 1971) and will simultaneously produce bremsstrahlung X-rays. As noted by Koch and Motz (1959) in their review of bremsstrahlung phenomena, and as discussed in Section 1 of this paper, the directivity and polarisation of these thick target X-rays depend on the collisional scattering of the electrons in the target. An accurate calculation of the multiple scattering and energy loss of an electron beam in a thick plasma target is beyond the scope of this paper but an approximate scattering model will suffice to demonstrate the effect of the scattering on the bremsstrahlung emission.

Elwert and Haug (1971) and Haug (1972a) have shown that even at photon energies of order 50 keV, electrons of several hundred keV may contribute significantly to the directivity and polarisation of the X-ray burst in certain directions. This is due to the presence in the differential bremsstrahlung cross-sections of relativistic corrections of order $\beta = v/c$, where v and c are the velocities of the electron and of light respectively. (The cross-section contains a factor $(1-\beta\cos\chi)^4$ where χ defines the photon emission direction – Elwert and Haug, 1971). However, the corrections to the Coulomb scattering cross-section for relativistic dynamical effects are only of order β^2 (Darwin, 1913) and so may be neglected as a first approximation to the scattering problem. In a general Coulomb collision, a particle of mass m_1, charge q_1, is incident with

velocity v in a medium containing particles of mass m_2 charge q_2, at rest and of density n_2 (cm^{-3}). Integration over all possible impact parameters up to a cut-off at b_0 yields the following equations describing the mean rates of energy loss and of scattering for the incident particle (cf. Spitzer, 1962)

$$\frac{\mathrm{d}E}{\mathrm{d}t} = \frac{-2\pi(q_1q_2)^2\Lambda}{E}\frac{m_1}{m_2}n_2v \tag{1}$$

and

$$\frac{\mathrm{d}v_{\|}}{\mathrm{d}t} = \frac{-\pi(q_1q_2)^2\Lambda}{E}\left(1+\frac{m_1}{m_2}\right)n_2v^2, \tag{2}$$

where E is the energy of the incident particle, v the corresponding total velocity and $v_{\|}$ the component of this velocity parallel to the original direction of motion. (Λ is the usual Coulomb logarithm $\simeq \log_e(2Eb_0/e^2)$). Collective effects due to interaction of the plasma and the beam as a whole are neglected since the beam is dilute compared to the chromospheric plasma (cf. Brown, 1971). In the case of an electron, mass m, traversing an ionised plasma of pure hydrogen, proton density $n_p(\mathrm{cm}^{-3})$, it follows that, if M is the proton mass,

$$\frac{\mathrm{d}E}{\mathrm{d}t} = \left(\frac{\mathrm{d}E}{\mathrm{d}t}\right)_{\mathrm{ep}} + \left(\frac{\mathrm{d}E}{\mathrm{d}t}\right)_{\mathrm{ee}} = \frac{-2\pi e^4\Lambda}{E}n_{\mathrm{p}}v\left(1+\frac{m}{M}\right)$$

so that

$$\frac{\mathrm{d}E}{\mathrm{d}t} \approx \frac{-2\pi e^4\Lambda}{E}n_{\mathrm{p}}v. \tag{3}$$

Similarly

$$\frac{\mathrm{d}v_{\|}}{\mathrm{d}t} \approx \frac{-3\pi e^4\Lambda}{E^2}n_{\mathrm{p}}v^2. \tag{4}$$

Thus both ambient electrons and protons produce scattering of the incident electrons but only ambient electrons contribute significantly to the energy loss.

It must be emphasised at this point that Equations (3) and (4) describe the *mean* rates of change of E and of $v_{\|}$ for the electrons of an incident beam and neglect the dispersions about these means. The accuracy with which these mean rates represent the modification of the electron velocity distribution by collisions will decrease as the scattering and energy loss (and their dispersions) become very great. Thus the following analysis will only approximate the electron beam velocity distribution in the thick target. As will be seen shortly, however, the analysis does represent the chief properties of the thick target adequately for an assessment of their effect on the X-ray emission.

If the electron beam penetrates a plane parallel stratified plasma such as the chromosphere, then the scattering of an average beam electron may conveniently be described in terms of a coordinate z normal to the atmospheric strata and directed into the plasma (i.e. downward). Then the mean electron energy may be expressed as a function $E(z)$ while the scattering is measured in terms of the angle $\theta(z)$ which the

mean electron velocity makes with the z axis at that point (cf. Figure 2). A more convenient quantity in many equations will be $\mu = \cos\theta$.

Equations (3) and (4) are thus the macroscopic equations of energy and momentum loss for the beam electrons, expressed in terms of the mean values of E and of $v_{\parallel}$. With this interpretation, Equation (4) may be resolved to give the z component of the mean momentum loss equation, viz.

$$\frac{\mathrm{d}v_z}{\mathrm{d}t} = \cos\theta \frac{\mathrm{d}v_{\parallel}}{\mathrm{d}t} = \frac{v_z}{v}\frac{\mathrm{d}v_{\parallel}}{\mathrm{d}t}. \tag{5}$$

(N.B. $v_{\parallel}$ signifies the component of v parallel to the original velocity and must not be confused with the common useage of the component parallel to the magnetic field.) A convenient change of independent variable is from t to N defined by

$$N = \int_{-\infty}^{z(t)} n_p(z')\,\mathrm{d}z' \tag{6}$$

(i.e. N is the number of protons per cm^2 column vertically above z), so that

$$\mathrm{d}N = n_{\mathrm{p}}\,\mathrm{d}z = n_{\mathrm{p}} v_z\,\mathrm{d}t.$$

In terms of N, Equations (3) and (5) are thus, (using (4) and setting $2\pi e^4 \Lambda = K$),

$$\frac{\mathrm{d}E}{\mathrm{d}N} = -\frac{K}{E}\frac{v}{v_z} \tag{7}$$

and

$$\frac{\mathrm{d}v_z}{\mathrm{d}N} = \frac{-3}{2}\frac{K}{E^2}v. \tag{8}$$

Thus

$$\frac{3}{2}\frac{1}{E}\frac{\mathrm{d}E}{\mathrm{d}N} = \frac{1}{v_z}\frac{\mathrm{d}v_z}{\mathrm{d}N}$$

with solution

$$(E/E_0)^{3/2} = v_z/v_{z_0} \tag{9}$$

where the suffix 0 refers to values at $N=0$. Since $v_z/v_{z_0} = (v_z/v)/(v_{z_0}/v_0) \times (v/v_0) = \mu/\mu_0 \times \times (E/E_0)^{1/2}$ then from (9) it follows that

$$\mu/\mu_0 = E/E_0 \tag{10}$$

and on resubstituting this in (7) and (8) solutions are obtained for μ and E, viz.

$$\mu = \mu_0(1 - 3KN/\mu_0 E_0^2)^{1/3} \tag{11}$$

and

$$E = E_0(1 - 3KN/\mu_0 E_0^2)^{1/3}. \tag{12}$$

These two equations may be solved analytically to give the initial values μ_0 and E_0

corresponding to an electron of given μ, E at a given depth N, viz.

$$\mu_0 = \mu(1 + 3KN/\mu E^2)^{1/3} \tag{13}$$

and

$$E_0 = E(1 + 3KN/\mu E^2)^{1/3} \tag{14}$$

which will also be required in Section 3.

The content of Equations (11) and (12), illustrated in Figure 1, gives the required information on the decrease in energy and the increase in horizontal scattering undergone by an average beam electron as it penetrates the target. It may be seen that on average an electron will have suffered a 60° deflection by the time its energy has been reduced by 50%. Thus some electrons will still be contributing hard X-rays when their velocities are within 30° of horizontal, confirming the importance of scattering as discussed in Section 1. On the other hand, once the scattering has become very great, say $\theta = 80°$, then an electron retains only about 17% of its original energy and cannot contribute greatly to hard X-ray emission. The errors arising from the neglect of

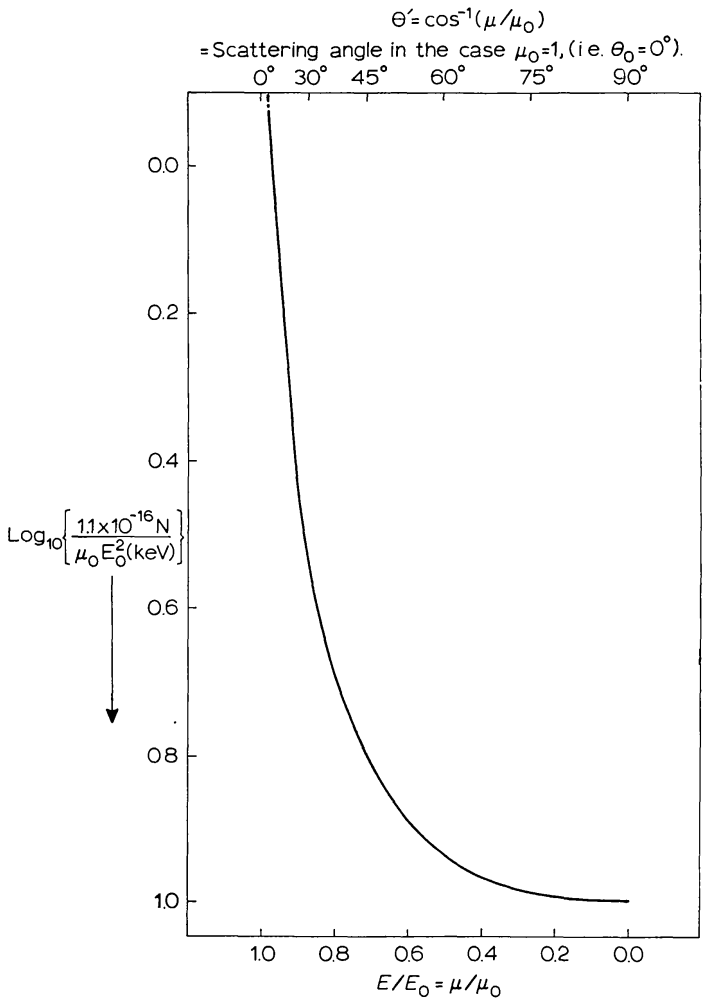

Fig. 1. Mean scattering and energy loss of electrons as a function of depth in the chromosphere. N = number of protons per cm^2 column above level in question. E, μ and E_0, μ_0 are the energy and the cosine of the pitch angle at this level and at the top of the atmosphere respectively.

dispersion in Equations (11) and (12) should, therefore, not be too severe in considering the X-ray emission since these errors are likely to be great only for electrons which have, in any case, lost most of their energy.

In addition to their direct relevance to this paper, Equations (11) and (12) are of general interest in connection with fast particles in the solar atmosphere. They extend the analysis of this problem by Schatzman (1965) who neglects scattering. In particular it is of interest to compare the energy loss Equation (12) with that obtained without scattering. In the latter case, $\mu = v_z/v$ in the energy Equation (7) is taken as constant, ($\mu = \mu_0$), and the solution is

$$E = E_0 (1 - 2KN/\mu_0 E_0^2)^{\frac{1}{2}}. \tag{15}$$

Comparison of Equations (12) and (15) shows that they make identical predictions of the energy loss rate for small N, viz.

$$E \approx E_0 (1 - KN/\mu_0 E_0^2) \quad (N \ll \mu_0 E_0^2/K).$$

For larger N, however, the energy goes to zero more rapidly when scattering is included as is seen by consideration of the depth of material N_s required to 'stop' (i.e. thermalise) a given electron. $N_s = \mu_0 E_0^2/2K$ when scattering is neglected while $N_s = \mu_0 E_0^2/3K$ on the basis of the scattering model developed above. (Even for an electron of $E_0 = 500$ keV, the latter value of N_s is about 2×10^{22} cm^{-2} which is low enough to guarantee that the whole thick target source is *optically* thin even at photon energies as low as 10 keV – Ohki, 1969).

3. Directivity and Polarisation of Thick Target Bremsstrahlung

Electrons injected into the chromosphere in the course of a flare will be guided in their downward paths by the flare magnetic field lines, about which they spiral. As stated in Section 1, in this paper the case of a purely vertical field is investigated in detail. Modification of the results by deviations from a vertical field are discussed in Section 4. Then the scattering angle θ introduced in Section 2 is identical with the electron pitch angle – i.e. the angle between the field Θ and the electron momentum $\mathbf{p}$ as in Figure 2. The other important direction involved in the emission is that of the emitted photon, momentum $\mathbf{q}$, making angle Θ with the *negative z* direction. (i.e. with $-\mathbf{H}$) as shown in Figure 2. Θ is then the heliocentric angular distance of the X-ray source from the disk centre ($\approx$CMD for small latitudes). A convenient coordinate system is one in which the xOz plane contains $\mathbf{H}$ and $\mathbf{q}$. The direction of $\mathbf{p}$ is then completely specified by its polar angles (θ, ϕ) with respect to this system, ϕ being the azimuth of $\mathbf{p}$, measured as in Figure 2. For an electron of initial momentum $\mathbf{p}$ emitting a photon of momentum $\mathbf{q}$, the bremsstrahlung cross-section depends on the photon energy ε (defined by $|\mathbf{q}|$), on the electron energy E(i.e. on $|\mathbf{p}|$) and on the angle χ between the directions $\hat{\mathbf{p}}$ and $\hat{\mathbf{q}}$. In terms of the angles of Figure 2, this is given by

$$\cos\chi = -\cos\theta\cos\Theta + \sin\theta\sin\Theta\cos\phi. \tag{16}$$

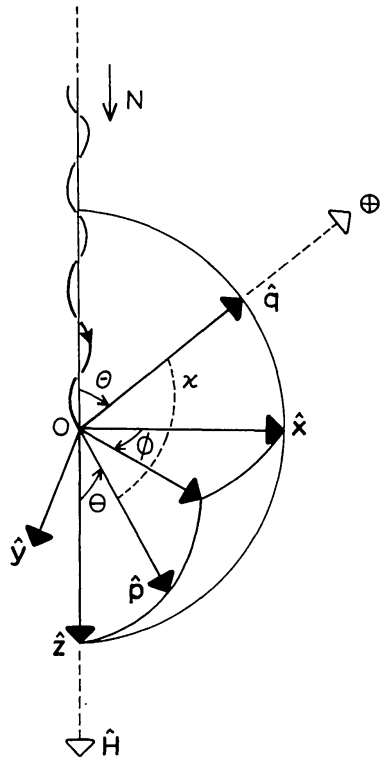

Fig. 2. Geometry of emission of a bremsstrahlung photon, momentum **q** by an electron of momentum **p** spiralling about field **H**.

In a 1 cm^3 volume about O, depth N, let the number of nonthermal electrons with kinetic energy between E and $E+\mathrm{d}E$ and with $\hat{\mathbf{p}}$ within solid angle $\mathrm{d}\Omega$ about (θ, ϕ) be

$$n(E, \theta, \phi, N)\,\mathrm{d}E\,\mathrm{d}\Omega\,.$$

If $\sigma''(E,\varepsilon, \chi)$ is the differential bremsstrahlung cross-section per unit photon energy ε and per unit solid angle about the direction $\hat{\mathbf{q}}$ of photon emission, then the nonthermal electrons in an interval $\mathrm{d}z$ of a vertical cylinder of $\mathrm{d}S$ cm^2 produce an X-ray flux at the Earth of

$$d^4I(\varepsilon, \Theta) = \left(\frac{r_0}{R}\right)^2 n(E, \theta, \phi, N)\, v(E)\,\mathrm{d}z\,\mathrm{d}S\,\mathrm{d}E\,\mathrm{d}\Omega n_p(N)\,\sigma''(E, \varepsilon, \chi) \tag{17}$$

(photons cm^{-2} s^{-1} per unit ε) where σ'' is in units of r_0^2 (r_0 being = classical electron radius, and $R=1$ AU). The total flux at the Earth from the $\mathrm{d}S$ cm^2 column ($\mathrm{d}I$ photons cm^{-2}s^{-1} per unit ε) is obtained by integration of (17) over the length of the column and over all electron energies, pitch angles and azimuths. (Photon absorption in the source is negligible as shown at the end of Section 2). Due to the rapid spiralling of the electrons $n \neq n(\phi)$ in fact and only σ'' need be integrated over ϕ, i.e. we can write $n(E, \theta, \phi, N) = n(E, \theta, N)$. Also, only energies $E \geqslant \varepsilon$ need be considered and, by Equations (11) and (12), no electrons with $\theta > \pi/2$ will be present.

On setting

$$n_p \, dz = dN$$
$$d\Omega = \sin\theta \, d\theta \, d\phi$$

and $\sin\theta \, d\theta = -d\mu$

then dI may be expressed as

$$dI(\varepsilon, \Theta) = (r_0/R)^2 \, dS \int_{N=0}^{\infty} \int_{E=\varepsilon}^{\infty} \int_{\mu=0}^{1} n(E, \theta, N) \, v(E) \times \times \left[\int_0^{2\pi} \sigma''(E, \varepsilon, \chi) \, d\phi \right] d\mu \, dE \, dN . \quad (18)$$

The cross-section σ'' may be expressed as the sum of σ''_1 and σ''_2, the cross-sections for emission of photons polarised parallel and perpendicular to the plane of emission (i.e. of $\hat{\mathbf{p}}$ and $\hat{\mathbf{q}}$) respectively. The necessary relativistic cross-sections have been given by Gluckstern and Hull (1953) and, following Elwert and Haug (1971), will be adopted here with a Coulomb correction factor (Elwert, 1939). In the presence of a magnetic field, however, the polarisation components of the total emission cannot be referred to a plane of photon emission since no such unique plane exists (due to the spiralling of the electrons), as noted by Haug (1972a). Haug shows that the polarisation may instead be referred to the plane containing the vectors $\mathbf{q}$ and $\mathbf{H}$ (i.e. the line of sight and the magnetic field) and further that in this case the polarisation 'intensity' is given by integrating over the distribution of the non-thermal electrons, with, in effect, a polarisation cross-section

$$\sigma''_p = (\sigma''_2 - \sigma''_1) \cos 2\psi . \quad (19)$$

The geometric factor $\cos 2\psi$, introduced by the spiralling, is given by

$$\cos 2\psi = \frac{(\mathbf{p} \times \mathbf{q}) \cdot (\mathbf{H} \times \mathbf{q})}{|\mathbf{p} \times \mathbf{q}| \, |\mathbf{H} \times \mathbf{q}|} . \quad (20)$$

With the geometry of Figure 2, a little analysis shows that $\cos\psi$ is given here by

$$\cos\psi = \frac{\sin\Theta \cos\theta + \cos\Theta \sin\theta \cos\phi}{\sin\chi} , \quad (21)$$

where χ is obtain from Equation (16).

From Equation (19) it follows that the *difference* in X-ray intensities between components polarised perpendicular and parallel to the plane defined by $\mathbf{H}$ and $\mathbf{q}$, from a dS cm^2 column of the thick target is

$$dI_p = dI_\perp - dI_\parallel$$
$$dI_p = \left(\frac{r_0}{R}\right)^2 dS \int_{N=0}^{\infty} \int_{E=\varepsilon}^{\infty} \int_{\mu=0}^{1} n(E, \theta, N) \, v(E) \left[\int_0^{2\pi} \sigma''_p \, d\phi \right] d\mu \, dE \, dN \quad (22)$$

while their sum is given by (18).

The form of $n(E, \theta, N)$ is determined by that of $n_0(E_0, \theta_0)$, the number density of injected electrons per unit energy and steradian at $N=0$, via the continuity equation. Since the guiding magnetic field is everywhere vertical and the system is assumed to have attained a steady state, the *vertical* flux of electrons in a given θ, E interval is constant. Thus

$$n(E, \theta, N) \sin\theta \, d\theta \, d\phi \, dE \, v \cos\theta = n_0(E_0, \theta_0) \sin\theta_0 \, d\theta_0 \, d\phi_0 \, dE_0 v_0 \cos\theta_0$$

i.e.

$$n(E, \theta, N) \, v(E) = n_0(E_0, \theta_0) \, v_0(E_0) \frac{\cos\theta_0}{\cos\theta} \frac{\sin\theta_0}{\sin\theta} \frac{\partial(E_0, \theta_0, \phi_0)}{\partial(E, \theta, \phi)}$$

or

$$n(E, \theta, N) \, v(E) = n_0(E_0, \theta_0) \, v_0(E_0) \frac{\cos\theta_0}{\cos\theta} \frac{\partial(E_0, \mu_0)}{\partial(E, \mu)}, \tag{23}$$

where E_0, μ_0 are expressed in terms of E, μ, N by Equations (13) and (14). By use of these latter equations it is found that the Jacobian is given by

$$\frac{\partial(E_0, \mu_0)}{\partial(E, \mu)} = \frac{1}{[1 + 3KN/\mu E^2]^{1/3}} = \frac{\mu}{\mu_0}. \tag{24}$$

Thus Equation (23) is simply

$$n(E, \theta, N) \, v(E) = n_0(E_0, \theta_0) \, v_0(E_0). \tag{25}$$

Substituting this expression into Equations (18) and (22) then integrating these over the region S of electron injection, the total burst intensity I and intensity difference $I_p = I_\perp - I_\parallel$ are given by

$$I(\varepsilon, \Theta) = \left(\frac{r_0}{R}\right)^2 \int_{N=0}^{\infty} \int_{E=\varepsilon}^{\infty} \int_{\mu=0}^{1} G(E_0, \theta_0) \left[\int_0^{2\pi} \sigma'' \, d\phi \right] d\mu \, dE \, dN \tag{26}$$

and

$$I_p(\varepsilon, \Theta) = \left(\frac{r_0}{R}\right)^2 \int_{N=0}^{\infty} \int_{E=\varepsilon}^{\infty} \int_{\mu=0}^{1} G(E_0, \theta_0) \left[\int_0^{2\pi} \sigma_p'' \, d\phi \right] d\mu \, dE \, dN, \tag{27}$$

where

$$G(E_0, \theta_0) = \int_S n_0(E_0, \theta_0) \, v_0(E_0) \, dS. \tag{28}$$

The form of $G(E_0, \theta_0)$, the total number of electrons injected per second per unit E_0 and per steradian about pitch angle θ_0 is determined by the acceleration mechanism which is unknown. In this paper it will be supposed that all the electrons have a Delta-function distribution at some small pitch angle θ_{00} before scattering occurs in the thick target, such as in the case of acceleration by a direct electric field (Sweet, 1969). On the matter of the electron distribution over energy E_0, definitive information is available only from hard X-ray burst spectral observations and not from theoretical models. In an analysis of thick target X-ray sources, Brown (1971) has shown in the

non-relativistic energy range that the flux spectrum $F(E_0)$ follows a power-law $\sim E_0^{-\delta}$ where δ is related to the index γ of the observed X-ray power-law $\sim \varepsilon_0^{-\gamma}$ by $\delta = \gamma + 1$. The relativistic deviation from this relation in the energy range considered here changes δ by less than $\frac{1}{2}$ and will be neglected. Observational results (Frost, 1969; Kane and Anderson, 1970) show that γ varies from 2 to 4 between various bursts, at values of ε less than some value ε_{00}, above which γ increases by at least 2. In most bursts, $\varepsilon_{00} \approx 100$ keV, but in large events this 'cut-off' may be as high as 500 keV (Cline *et al.*, 1968). In the deduction of these electron spectra, the mean value of the bremsstrahlung cross-section over photon emission direction was used. However, Elwert and Haug (1970) suggested that the relationship between the electron and X-ray energy spectra was insensitive to direction, a conclusion borne out by the detailed results of the present paper. (See Section 4 and also Figure 6). Conversely the directivity of the source is not sensitive to the electron spectrum so that the above power-law spectrum will be quite an adequate representation.

These data will be summarised here by adoption of the following form for $G(E_0, \theta_0)$

$$G(E_0, \theta_0) = F(E_0)\,\delta(\theta_0 - \theta_{00}), \tag{29}$$

where

$$F(E_0) = \begin{cases} AE_0^{-\delta_1}, & E_0 \leqslant E_{00} \\ AE_{00}^{\delta_2-\delta_1}E_0^{-\delta_2}, & E_0 \geqslant E_{00} \end{cases} \tag{30}$$

where A is a constant and $\delta(\theta_0 - \theta_{00})$ is the Delta function. When this form of G is substituted into Equation (27), the μ integration is zero everywhere except at $\theta = \theta_1$, the solution of

$$\theta_0(\theta_1, E, N) = \theta_{00}. \tag{31}$$

When $N < \mu_{00}E^2/2^{2/3}K$ this equation has three real roots for μ_1 of which two are eliminated by the requirement that $0 \leqslant \mu_1/\mu_{00} \leqslant 1$. The absolute intensity I of an X-ray burst, as given by Equation (26), is not of interest here as it depends on the quantity A in Equation (30), i.e. on the total number of injected electrons. Relative changes of $I(\varepsilon, \theta)$ with varying ε and Θ for a given burst are what is required and these may conveniently be expressed in terms of a dimensionless *directivity* $\boldsymbol{D}$ defined by

$$\boldsymbol{D} = I(\varepsilon, \Theta)/I(\varepsilon, 0). \tag{32}$$

Recalling the definition of Θ, it is seen that an increase of $\boldsymbol{D}$ with Θ corresponds to limb-brightening of bursts while a decrease implies a limb-darkening.

Similarly the quantity I_p (Equation (27)) is best expressed in terms of the *degree of polarisation* $\boldsymbol{P}$ defined by

$$\boldsymbol{P} = \frac{I_\perp - I_\parallel}{I_\perp + I_\parallel} = \frac{I_p(\varepsilon, \Theta)}{I(\varepsilon, \Theta)}. \tag{33}$$

(It may be emphasised at this point that $I_\parallel$ is the intensity of the component polarised in the plane of **H** and **q**, which, in the case of a purely vertical field **H** is the plane

containing the Earth, the centre of the solar disk and the burst source.) The integrals in (26) and (27) may themselves be reduced to dimensionless form by means of the substitutions

$$\begin{aligned} k &= E/mc^2 \\ \varrho &= \varepsilon/mc^2 \\ \nu &= 3KN/(mc^2)^2 , \end{aligned} \tag{34}$$

where mc^2 is the electron rest energy. It then follows finally that $\boldsymbol{D}$ and $\boldsymbol{P}$ are given by

$$\boldsymbol{D}(\varepsilon, \Theta) = \frac{\int_{\nu=0}^{\infty}\int_{k=\varrho}^{\infty} F(k_0(k,\theta_1))\left[\int_0^{2\pi}\sigma''(k,\varepsilon,\chi_1)\,\mathrm{d}\phi\right]\mathrm{d}k\,\mathrm{d}\nu}{\int_{\nu=0}^{\infty}\int_{k=\varrho}^{\infty} F(k_0(k,\theta_1))\left[\int_0^{2\pi}\sigma''(k,\varepsilon,\chi_2)\,\mathrm{d}\phi\right]\mathrm{d}k\,\mathrm{d}\nu} \tag{35}$$

and

$$\boldsymbol{P}(\varepsilon, \Theta) = \frac{\int_{\nu=0}^{\infty}\int_{k=\varrho}^{\infty} F(k_0(k,\theta_1))\left[\int_0^{2\pi}\sigma_p''(k,\varepsilon,\chi_1)\,\mathrm{d}\phi\right]\mathrm{d}k\,\mathrm{d}\nu}{\int_{\nu=0}^{\infty}\int_{k=\varrho}^{\infty} F(k_0(k,\theta_1))\left[\int_0^{2\pi}\sigma''(k,\varepsilon,\chi_1)\,\mathrm{d}\phi\right]\mathrm{d}k\,\mathrm{d}\nu} , \tag{36}$$

where F is given by (30), $k_0(k, \theta_1)$ by (14), θ_1 being the solution of (31), and where

$$\begin{aligned} \cos\chi_1 &= -\cos\theta_1\cos\Theta + \sin\theta_1\sin\Theta\cos\phi \\ \cos\chi_2 &= -\cos\theta_1 . \end{aligned} \tag{37}$$

The integrals contained in (35) and (36) were computed numerically for a range of values of the variables ε and Θ, and of the parameters θ_{00}, E_{00}, δ_1 and δ_2 with the results described and discussed in the following section.

4. Results and Discussion

Results for $\boldsymbol{D}(\varepsilon, \Theta)$ and $\boldsymbol{P}(\varepsilon, \Theta)$ were computed for three values of the photon energy ε, viz. 10, 50 and 150 keV and for values of Θ from 0° (disk centre) up to 90° (the limb) at 15° intervals. (It is a notable feature of this model, resulting from the symmetry of a vertical field that $\boldsymbol{D}$ and $\boldsymbol{P}$ depend only on the heliocentric angular distance Θ of the burst, for each ε). The main integrations were performed with the initial pitch angle θ_{00} set $=0°$. This could have been used to simplify the analysis of Section 3 from the outset but the more general case is required later. $F(E_0)$, the electron flux spectrum, was taken to be $\sim E_0^{-4}$ up to $E_{00}=100$ keV steepening to $\sim E_0^{-6}$ above this energy (c.f. Frost, 1969). Though the results obtained were modified on varying the

parameters θ_{00}, E_{00}, δ_1 and δ_2, as discussed more fully later, the changes were always small.

For comparison purposes, similar calculations were carried out for a model in which scattering was neglected by setting $\theta=\theta_{00}$ for all E, N instead of $\theta=\theta_1(\theta_{00}, E, N)$ as given by Equation (31). In both the models, with and without scattering, the thick target modification of the electron *energy* distribution, as given by Equation (12), was, however included (cf. Brown, 1971). Figure 3 shows the results for $\boldsymbol{D}$ in each model. In the absence of scattering, bursts brighten monotonically from the disk centre to the limb, the limb to centre intensity ratio being about 4.5 at 10 keV and about 6.0 at both 50 and 150 keV photon energies. As anticipated in Section 1, this anisotropy is considerably modified when scattering is introduced. From Figure 3 it can be seen that, although the form of $\boldsymbol{D}$ still indicates a limb brightening of bursts, the limb to centre ratio has been reduced to less than 2.0 at 10 keV. Scattering has a diminishing effect on the directivity at higher photon energies. Thus, at 50 keV, the limb brightening has been reduced from 6.0 to 3.0 while at 150 keV the ratio is scarcely reduced below its value with no scattering present. In Section 1 it was emphasised that adequate observational data on $\boldsymbol{D}$ are only available at present in the 1–6 keV photon range. Thus Figure 3 cannot be compared with observations except to say that the anisotropy of the non-thermal bremsstrahlung at 1–6 keV predicted by extrapolation of Figure 3, when combined with a large thermal component (Kahler and Kreplin, 1971) lies well within the statistical limits set by observations (Drake, 1971).

In Figure 4 the results for the polarisation $\boldsymbol{P}(\varepsilon, \Theta)$ are shown for models with and without scattering. In all cases there is zero polarisation for bursts at the disk centre ($\Theta=0°$). This is so since no preferred plane can exist when observations are made looking down the vertical field lines. Away from the disk centre $\boldsymbol{P}$ increases in magnitude, rising as high as -0.8 at the limb for 10 and 50 keV photons and to -0.6 for 150 keV photons from the model without scattering. The effect of scattering is, of course, to reduce $\boldsymbol{P}$, the greatest reduction being at low photon energies. Thus the maximum polarisation is reduced to -0.3 at 10 keV, to -0.35 at 50 keV and to -0.45 at 150 keV, these maxima occurring at or near the limb (Figure 4). By the definition of $\boldsymbol{P}$, Equation (33), its negative value in all cases studied here implies that the plane of maximum intensity contains the magnetic field and the line of sight. In this model, therefore, a maximum count rate should occur when a plane-polarising detector is oriented along the solar radius through the X-ray flare.

Tindo *et al.* (1970, 1972a, b) have reported observations of flare X-ray polarisation at around 15 keV from the satellites Intercosmos 1 and 4. Their most recent report (1972b) contains reasonably exact data on $\boldsymbol{P}(\pm<0.1)$ for three bursts and, furthermore, finds that the plane of polarisation does indeed pass through the flare and the disk centre, to within 10° in each case, in agreement with the above prediction. As a further comparison with the model described here, Figure 5 shows the observed values of $\boldsymbol{P}$, against distance Θ from the disk centre, for these three bursts and also for two further bursts (Tindo *et al.*, 1970) for which the results are less precise. Superposed are

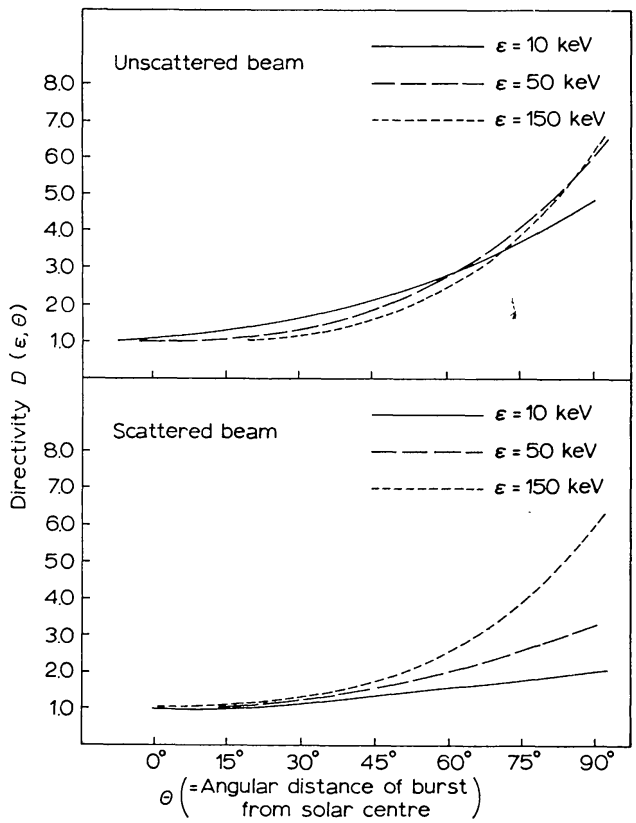

Fig. 3. Directivity of emission from continuous injection model, with and without scattering, as a function of photon energy ε and of angular heliocentric distance Θ of source.

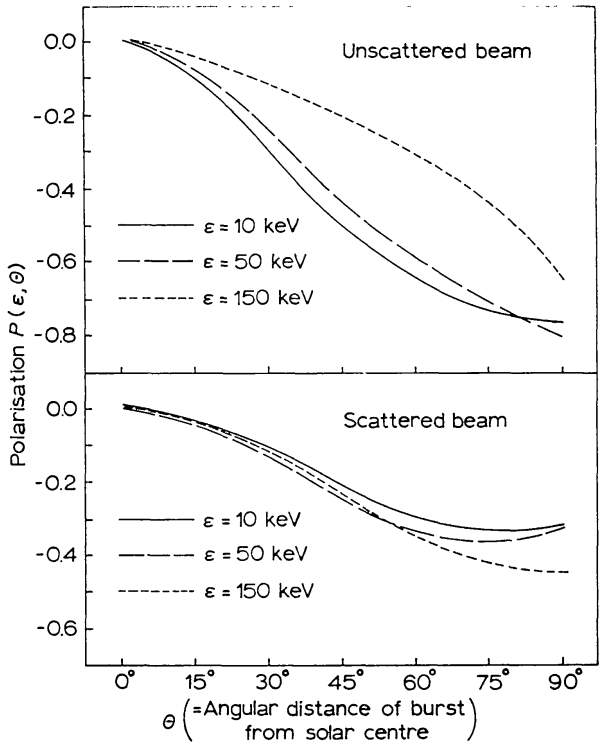

Fig. 4. Polarisation of emission from continuous injection model, with and without scattering, as a function of photon energy ε and of angular heliocentric distance Θ of source.

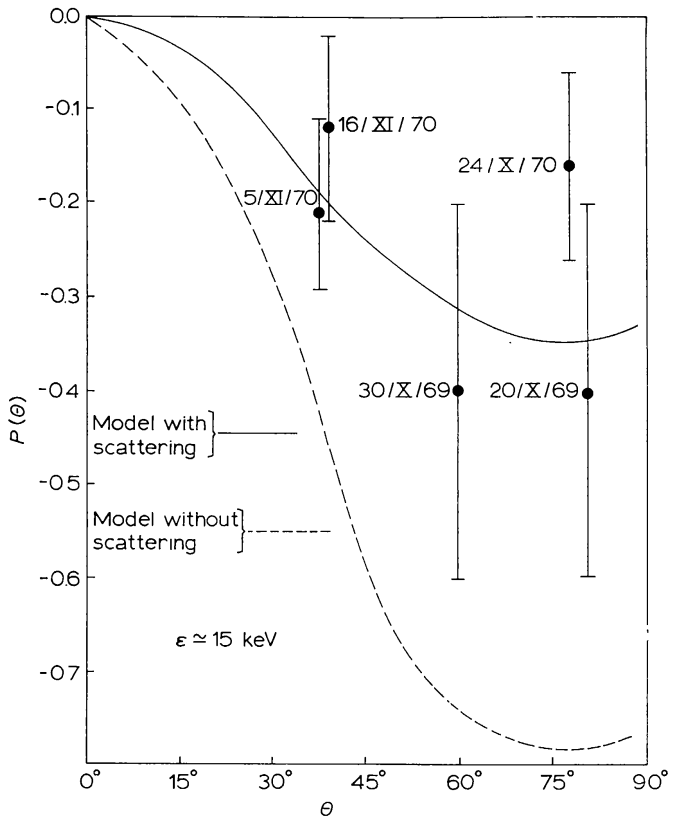

Fig. 5. Comparison of the magnitude $|\boldsymbol{P}|$ of the predicted polarisation at 15 keV from the continuous injection model (with and without scattering) and the observations of Tindo *et al.* (1970, 1972a, b).

the curves predicted by the continuous injection model with and without scattering. Evidently the data are quite consistent with the model including scattering though the error bars are too large for the results to be conclusive as yet. Tindo *et al.* (1972b) find that the observed polarisation is less than their predictions for the continuous injection model but this can be accounted for by their neglect of scattering as is readily seen from Figure 5. Observed values of $|\boldsymbol{P}|$ are in fact a little lower than those predicted even with scattering. This may be partly due to a superposed thermal component but could also indicate deviation of the magnetic field from the vertical in the X-ray flare, (cf. Strauss and Papagiannis, 1971), which would reduce the anisotropy in the overall electron velocity distribution. On this interpretation, measurement of $|\boldsymbol{P}|$ at higher photon energies could prove to be a useful probe of the flare field since high energy electrons will penetrate the atmosphere, and hence the field structure, more deeply.

Though exact predictions for the *impulsive injection model* will require a detailed analysis, comparable to that in Section 3, some qualitative conclusions may be stated here for comparison purposes. Firstly, the predominance of large pitch angles, imposed by the trapping requirement, will result in a plane of bremsstrahlung polarisation perpendicular to the magnetic field (as opposed to parallel to it for the continuous model) – cf. Haug (1972a). As regards the direction of the field in the impulsive model, Brown (1972) has shown that electrons of lowest energy are confined near the

top of the trap where the field is almost horizontal while those of high energy emit X-rays principally in the near vertical trap limbs. For low energy X-rays, therefore, the field is effectively horizontal and so its projection could be arbitrarily oriented on the solar disk, though an east-west direction might be favoured if bipolar spots were involved (cf. Takakura and Kai, 1966). With such a geometry it is unlikely that the plane of polarisation (normal to the field) would happen to pass through the disk centre as it was observed to do for each of three bursts by Tindo *et al.* (1972b). For high energy X-rays on the other hand the near vertical field implies a plane of polarisation perpendicular to the solar radius through the X-ray source, contrary to observation. Though the 15 keV photons observed by Tindo *et al.* are intermediate between these low and high energy cases, it is therefore hard to see how the impulsive model could be reconciled with these observations. Future data on the plane of polarisation at different wavelengths should settle any uncertainty in this problem.

Considering again the continuous injection model, some checks may be made on the sensitivity of the results of this paper to the assumptions of the model. The results for the model without scattering are found to compare satisfactorily with those of Elwert and Haug (1971) and of Haug (1972a) in their case of zero pitch angle. (In making this comparison it must be recalled that the flux spectrum $F(E_0)$ of the electrons *at injection* into a thick target is two powers steeper than their effective flux spectrum in the source region – Brown (1971) – which is that considered by Elwert and Haug). Considering the thick target model, Haug (1972a, b) has suggested that a $\cos^2\theta$ distribution of electrons over pitch angle might roughly represent the scattered beam. Computations by Haug (1972b) based on this distribution do indeed yield results for $\boldsymbol{D}$ and $\boldsymbol{P}$ similar to those in Figures 3 and 4 (scattered case) except at high photon energies. At these higher energies Haug's results show a greater reduction in $\boldsymbol{D}$ and $\boldsymbol{P}$ due to the spread of pitch angles than was found in the present paper. This discrepancy arises since Haug has neglected the energy dependence of scattering in the target which would affect high energy electrons less than low energy ones. On the other hand, the approximate agreement between the present work and that of Haug (1972b) indicates that the form of $\boldsymbol{D}$ and $\boldsymbol{P}$ is not highly sensitive to the pitch angle distribution involved. The approximate model of thick target scattering, derived in Section 2, should therefore certainly be adequate for the present purpose.

The effect of varying the parameters θ_{00}, E_{00}, δ_1 and δ_2 from the values used in Figures 3 and 4 was also investigated. It was found that increase of θ_{00} from 0° had the predictable effect of reducing the range of variation of both $\boldsymbol{P}$ and $\boldsymbol{D}$ by producing a more nearly isotropic velocity distribution. For values of θ_{00} up to about 20°, however, the changes were less than 5%. Overall hardening of the electron spectrum by decreasing both δ_1 and δ_2 resulted in a somewhat decreased directivity and polarisation especially for 50 and 150 keV photons. This rather unexpected result is due to the increased contribution of photons by electrons well above the bremsstrahlung threshold energy. Emission near the threshold is particularly directional in respect of photons emitted in the backward hemisphere (Haug, 1972b). A similar interpretation applies to the reduction of $\boldsymbol{P}$ and of $\boldsymbol{D}$ (at $\varepsilon = 50$ and 150 keV) produced by increasing

E_{00} to 500 keV or, equivalently, by decreasing δ_2 to 4. In all cases, however, reasonable variations of the parameters produced only modest changes in $\boldsymbol{D}$ and $\boldsymbol{P}$ and in no case affected the qualitative conclusions reached above.

Finally, integration of equation (26) for $I(\varepsilon, \Theta)$ with $\delta_1 = \delta_2 = 4$ was used to test the dependence of the photon spectrum on direction of observation. Figure 6 shows the values of I at four values of Θ (viz. 0°, 30°, 60° and 90°) for each photon energy (i.e. 10, 50 and 150 keV). These results may be compared with the spectrum obtained when directional effects are neglected, i.e. when a cross-section averaged over the photon emission direction is taken. Brown (1971) has shown that when the non-relativistic Bethe-Heitler cross-section is adopted, the photon flux spectrum corresponding to an electron flux distribution $\sim E_0^{-4}$ at injection into a thick target is $\sim \varepsilon^{-3}$. In Figure 6 the best power-law spectral fit is drawn at each value of Θ. For bursts near the disk centre this fit is within $\frac{1}{2}$ a power of the mean non-relativistic photon spectrum while nearer the limb deviation is considerably smaller still. (This is so since relativistic corrections to the cross-section are greatest in the backward and forward photon directions, i.e. $\Theta \approx 0°$ and $\Theta \approx 180°$, the latter being unobserved here as it corresponds to a burst behind the limb). Thus the photon spectrum is not sensitive to the emission direction and conversely, the source electron spectrum required to produce an observed X-ray spectrum is insensitive to the direction of observation. It follows that directional effects may safely be neglected in assessing electron spectra from hard X-ray flare spectra, as assumed by Brown (1971).

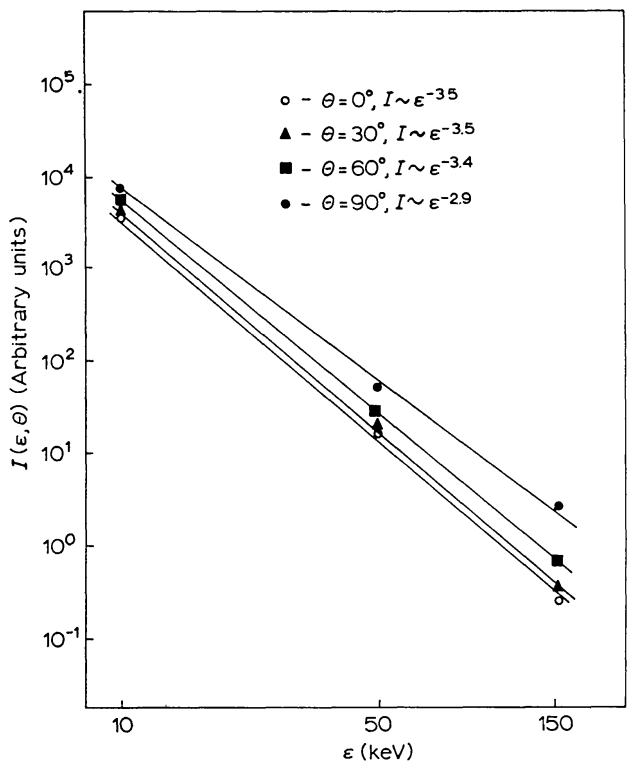

Fig. 6. Dependence of the X-ray spectrum on the direction of observation. Best power law fit is shown for each direction.

Acknowledgements

The author wishes to express his thanks to Professor P. A. Sweet and to Dr E. Haug for helpful discussion both of the manuscript and of the problem itself. He also wishes to acknowledge with gratitude the hospitality of Professor G. Elwert and the support of a Deutscher Akademischer Austauchsdienst Stipend during the period November 1971 to March 1972 at the Lehrstuhl für Theoretische Astrophysik der Universität Tübingen, West Germany. Thanks are also due to all members of the Department of Astronomy, University of Glasgow, whose consideration made this leave possible, and to Herr W. Kipp whose assistance with the computations involved in the problem was invaluable.

References

Acton, L. W.: 1968, *Astrophys. J.* **152**, 305.
Benz, A. O. and Gold, T.: 1971, *Solar Phys.* **21**, 157.
Brown, J. C.: 1971, *Solar Phys.* **18**, 489.
Brown, J. C.: 1972, *Solar Phys.* **25**, 158.
Cheng, C. C.: 1972, *Solar Phys.* **22**, 178.
Cline, T. L., Holt, S. S., and Hones, E. W.: 1968, *J. Geophys. Res.* **73**, 434.
Darwin, C. G.: 1913, *Phil. Mag.* **25**, 201.
Drake, J. F.: 1971, *Solar Phys.* **16**, 152.
Elwert, G.: 1939, *Ann. Physik.* **34**, 178.
Elwert, G.: 1968, in K. O. Kiepenheuer (ed.), 'Structure and Development of Solar Active Regions', *IAU Symp.* **35**, 144.
Elwert, G. and Haug, E.: 1970, *Solar Phys.* **15**, 234.
Elwert, G. and Haug, E.: 1971, *Solar Phys.* **20**, 413.
Frost, K. J.: 1969, *Astrophys. J.* **158**, L 159.
Gluckstern, R. L. and Hull, M. H.: 1953, *Phys. Rev.* **90**, 1030.
Haug, E.: 1972a, *Solar Phys.* **25**, 425.
Haug, E.: 1972b, private communications.
Hudson, H. S.: 1971, private communication.
de Jager, C. and Kundu, M. R.: 1963, *Space Res.* **3**, 836.
Kahler, S. W. and Kreplin, R. W.: 1971, *Astrophys. J.* **168**, 531.
Kane, S. R. and Anderson, K. A.: 1970, *Astrophys. J.* **162**, 1003.
Koch, H. W. and Motz, J. W.: 1959, *Rev. Mod. Phys.* **31**, 920.
Korchak, A. A.: 1967a, *Soviet Astron.-AJ* **11**, 258.
Korchak, A. A.: 1967b, *Soviet Phys. Doklady* **12**, 192.
Lin, R. P. and Hudson, H. S.: 1971, *Solar Phys.* **17**, 412.
Ohki, K.: 1969, *Solar Phys.* **7**, 260.
Pinter, Š.: 1969, *Solar Phys.* **8**, 142.
Schatzman, E.: 1965, in C. de Jager (ed.), *The Solar Spectrum,* D. Reidel Publishing Company, p. 313.
Spitzer, L.: 1962, *Physics of Fully Ionised Gases*, Interscience.
Strauss, F. M. and Papagiannis, M. D. A.: 1971, *Astrophys. J.* **164**, 369.
Sturrock, P. A.: 1968, in K. O. Kiepenheuer (ed.), 'Structure and Development of Solar Active Regions', *IAU Symp.* **35**, 471.
Sweet, P. A.: 1969, *Ann. Rev. Astron. Astrophys.* **7**, 149.
Syrovatskii, S. I. and Shmelva, O. P.: 1972, to appear in *Soviet Astron.-AJ.*
Takakura, T. and Kai, K.: 1966, *Publ. Astron. Soc. Japan* **18**, 57.
Takakura, T. and Scalise, E.: 1970, *Solar Phys.* **11**, 434.
Tindo, I. P., Ivanov, V. D., Mandelstam, S. L., and Shuryghin, A. I.: 1970, *Solar Phys.* **14**, 204.
Tindo, I. P., Ivanov, V. D., Mandelstam, S. L., and Shuryghin, A. I.: 1972a, *Solar Phys.* **24**, 429.
Tindo, I. P., Valníček, B., Livshits, M. A., Ivanov, V. D.: 1972b, Lebedev Physical Institute, Laboratory of Spectroscopy, – Preprint No. 43.
Zirin, H., Pruss, G., and Vorpahl, J.: 1971, *Solar Phys.* **19**, 463.